processes

MDPI

Article

An Integrated Design Method for Used Product Remanufacturing Process Based on Multi-Objective Optimization Model

Chao Ke [1], Yanxiang Chen [2], Muyang Gan [3], Yang Liu [4,*] and Qunjing Ji [1,*]

[1] School of Art and Design, Wuhan Institute of Technology, Wuhan 430205, China; 22121401@wit.edu.cn
[2] School of Mechanical and Electrical Engineering, Wuhan City Polytechnic, Wuhan 430064, China; chenyanx@whcp.edu.cn
[3] College of Intelligent Manufacturing, Hubei Engineering Institute, Huangshi 435000, China; mygan1111@163.com
[4] Department of Mechanical and Electrical Engineering, Shihezi University, Shihezi 832003, China
* Correspondence: liuyang2024@shzu.edu.cn (Y.L.); 22121402@wit.edu.cn (Q.J.)

Abstract: The design for the remanufacturing process (DFRP) is a key part of remanufacturing, which directly affects the cost, performance, and carbon emission of used product remanufacturing. However, used parts have various failure forms and defects, which make it hard to rapidly generate the remanufacturing process scheme for simultaneously satisfying remanufacturing requirements regarding cost, performance, and carbon emissions. This causes remanufactured products to lose their energy-saving and emission-reduction benefits. To this end, this paper proposes an integrated design method for the used product remanufacturing process based on the multi-objective optimization model. Firstly, an integrated DFRP framework is constructed, including design information acquisition, the virtual model construction of DFRP solutions, and the multi-objective optimization of the remanufacturing process scheme. Then, the design matrix, sensitivity analysis, and least squares are applied to construct the mapping models between performance, carbon emissions, cost, and remanufacturing process parameters. Meanwhile, a DFRP multi-objective optimization model with performance, carbon emission, and cost as the design objectives is established, and a teaching–learning based adaptive optimization algorithm is employed to solve the optimization model to acquire a DFRP solution satisfying the target information. Finally, the feasibility of the method is verified by the DFRP of the turbine blade as an example. The results show that the optimized remanufacturing process parameters reduce carbon emissions by 11.7% and remanufacturing cost by USD 0.052 compared with the original process parameters, and also improve the tensile strength of the turbine blades, which also indicates that the DFPR method can effectively achieve energy saving and emission reduction and ensure the performance of the remanufactured products. This can greatly reduce the carbon emission credits of the large-scale remanufacturing industry and promote the global industry's sustainable development; meanwhile, this study is useful for remanufacturing companies and provides remanufacturing process design methodology support.

Keywords: remanufacturing process; multi-objective optimization; carbon emission; turbine blade

Citation: Ke, C.; Chen, Y.; Gan, M.; Liu, Y.; Ji, Q. An Integrated Design Method for Used Product Remanufacturing Process Based on Multi-Objective Optimization Model. *Processes* **2024**, *12*, 518. https://doi.org/10.3390/pr12030518

Academic Editors: Luigi Maria Galantucci and Diane Mynors

Received: 27 January 2024
Revised: 23 February 2024
Accepted: 27 February 2024
Published: 4 March 2024

1. Introduction

With the increasing problem of global warming, it has become an urgent and important issue to reduce carbon emissions in the life cycle of products. Remanufacturing is an essential industrial process of the value recovery method, which can increase the utilization rate of used products and reduce carbon emissions [1–3]. The remanufacturing process is a vital step that directly impacts the performance, carbon emission, and cost of used product remanufacturing [4].

Although the remanufacturing process has tremendous benefits, there are uncertainties in the failure characteristics and quality of used products, making it difficult to develop a reasonable remanufacturing process scheme to achieve the appropriate performance and cost requirements. Furthermore, the remanufacturing process of used products consumes water, materials, energy, etc. If the remanufacturing process scheme is not reasonable, it will lead to excessive material and energy consumption and result in a large amount of carbon emissions. This will result in the elimination of the energy-saving and emission-reduction advantages of remanufacturing. Therefore, it is necessary to design a rational remanufacturing process scheme targeting remanufactured product performance, cost, and remanufacturing carbon emissions. To address this problem, many scholars have conducted research related to the DFRP. Ke et al. [5] proposed an integrated design method for remanufacturing processes based on performance demand, which generated the remanufacturing process scheme for satisfying the remanufacturing performance. Chen et al. [6] proposed a knowledge-based method for remanufacturing process planning, which also aimed to improve the efficiency of process planning and realized the inheritance and evolvability of process planning knowledge. Jiang et al. [7] presented a hybrid method combining rough set (RS) and cased-based reasoning (CBR) for remanufacturing process planning, which was feasible and effective for the rapid generation of sound process planning for remanufacturing. Jiang et al. [8] proposed a data-driven ecological performance evaluation method for the remanufacturing process, which considered the energy-saving rate, remanufacturing process cost, and rate of remanufacturing. Jiang et al. [9] proposed an energy-efficient method for the laser remanufacturing process, which could reduce the energy consumption and cost of the laser remanufacturing process. The literature mentioned above shows that many scholars have conducted research on the remanufacturing processes from cost reduction, knowledge reuse, energy efficiency, performance requirements, etc. Undoubtedly, these studies provide great help in the intelligent generation and sustainability of the remanufacturing processes.

However, none of this research has taken into account the intrinsic links between remanufacturing costs, carbon emissions, and remanufactured product performance and remanufacturing process parameters, and is unable to provide a comprehensive remanufacturing process scheme that meets all three remanufacturing requirements. The remanufacturing process consumes a lot of materials and energy, which not only creates carbon emissions, but also costs the company money. The remanufacturing process scheme directly affects used product remanufacturing, determining the size of the carbon footprint and cost. In addition, the remanufacturing process not only affects the remanufacturing cost and carbon emissions, but also affects the performance of remanufactured products. Variability in remanufacturing process parameters will change the performance of remanufactured products. In order to develop a reasonable remanufacturing process scheme, it is necessary to construct a mapping correlation between the remanufacturing process parameters and the above-mentioned objectives in order to successfully implement used product remanufacturing.

For developing suitable remanufacturing process schemes to satisfy the remanufacturing requirements, it is essential to establish the mapping relationship between remanufacturing process parameters and remanufacturing carbon emissions, cost, and performance, and much research has been carried out in this area, for example, regarding the design method for a used product remanufacturing scheme considering carbon emission [10], reliability and cost optimization for remanufacturing process planning [11], an energy and time prediction model for the remanufacturing process [12], and the economic modeling of robotic disassembly for remanufacturing [13]. These studies analyzed the impact of the remanufacturing processes on carbon emissions, cost, and time. However, this research did not simultaneously consider the impact of process parameters on the performance of remanufactured products, which do not guarantee the reliability of the remanufactured product. To achieve this synergistic optimization of carbon emission, cost, and performance, it is

necessary to develop a mathematical model between process parameters, remanufacturing cost, carbon emission, and performance.

Currently, some studies have analyzed the relationship between remanufacturing process and performance, cost, and carbon emission. Existing research has mainly focused on remanufacturing process optimization from sustainability aspects [14], the optimization of remanufacturing process routes oriented toward eco-efficiency [15], an integrated optimization control method for the remanufacturing assembly system [16], and multi-process-routes-based re-manufacturability assessment [17]. These studies investigated the impact of remanufacturing processes on factors such as quality, cost, and carbon emissions. Although they analyzed the relationship between the three and the remanufacturing process, they did not comprehensively construct an accurate mathematical mapping model, which is not conducive to optimizing the remanufacturing process. For the properties of remanufactured products including hardness, tensile strength, bending strength, etc., in an axiomatic design theory, the mathematical model among process parameters and properties can be characterized by a process matrix (AD) [18], whereas sensitivity analysis enables one to analyze the influencing relationship between two variables [19]. Therefore, this method can be used to analyze the correlation between remanufacturing process parameters and remanufacturing carbon emissions. Otherwise, the least squares method can fit the curve function relationship between different variables [20], whereas this method is available for fitting the utilization of the mathematical correlation between process parameters and remanufacturing cost.

In addition, the DFRP is a multi-objective optimization problem as it needs to consider remanufacturing requirements such as cost, performance, and carbon emissions. Currently, there are many intelligent algorithms that have been developed to solve the multi-objective optimization problem. The most commonly used algorithms in the past included particle swarm algorithms [21], genetic algorithms [22], ant colony algorithms [23], etc. However, these methods cannot adaptively adjust the initial variable values and cannot guarantee the accuracy and stability of the optimization results. To deal with the limitations of the existing algorithms, we proposed an adaptive teaching-based optimization algorithm (ATLBO), which imitates the teaching process between the teacher and the students to adjust the teaching approach in achieving the goal of the rapid grasping of knowledge by the students [24]. This algorithm is able to adaptively optimize the initial parameters based on the optimization results, thus improving the accuracy of the optimization results.

In order to quickly generate a reasonable remanufacturing process scheme that satisfies the remanufacturing demands, this paper proposes an integrated design method for the remanufacturing process of used products. This method can establish the mapping relationship between the remanufacturing process parameters and remanufacturing cost, carbon emission, and performance, and use intelligent algorithms for the rapid solution of the remanufacturing process scheme. This method mainly contained three parts: DFRP framework establishment, multi-objective mapping model establishment, and DFRP optimization model establishment and solution. Especially, the main innovations of this research were as follows: (1) the construction of a design framework for the remanufacturing process based on a multi-objective optimization model from the perspective of remanufacturing carbon emission, cost, and performance. (2) Analyzing the mapping relationship model between remanufacturing process parameters and remanufacturing carbon emissions, cost, and performance. (3) The development of a DFRP optimization model and an intelligent solution to the optimal DFRP parameters. The DFRP solution of the turbine blade was used to verify the feasibility of the proposed method. Overall, the method provided an effective process design model for the remanufacturing of used products to reduce carbon emissions and remanufacturing costs, improve the performance of remanufactured products, and facilitate energy conservation and emission reduction in the remanufacturing industry for sustainable economic development.

2. Methods

2.1. Integrated Design Framework for Remanufacturing Process

The design for the remanufacturing process is to realize the performance of the remanufactured product, while the process engineer needs to consider the original structure, size, and performance constraints of the used products, as well as the enterprise cost requirements and environmental policy constraints. Therefore, process engineers need to adjust the remanufacturing process scheme based on actual customer demand, size constraints, and cost requirements. Firstly, the information needs to be collected including the original information on used products, customer demand information, remanufacturing company demand information, environmental policy information, etc. Then, the virtual model of the used product can be established based on the simulation technology, and the optimization model needs to be constructed for the remanufacturing process scheme. Finally, the ATLBO algorithm is to be applied to solve the multi-objective optimization model of the remanufacturing process solution, and the virtual simulation model will be simultaneously corrected and adjusted according to the solving results to verify the feasibility of the solving results. By continuous optimization and feedback adjustment, the optimal remanufacturing process scheme is acquired, and the specific design framework for the remanufacturing process is shown in Figure 1.

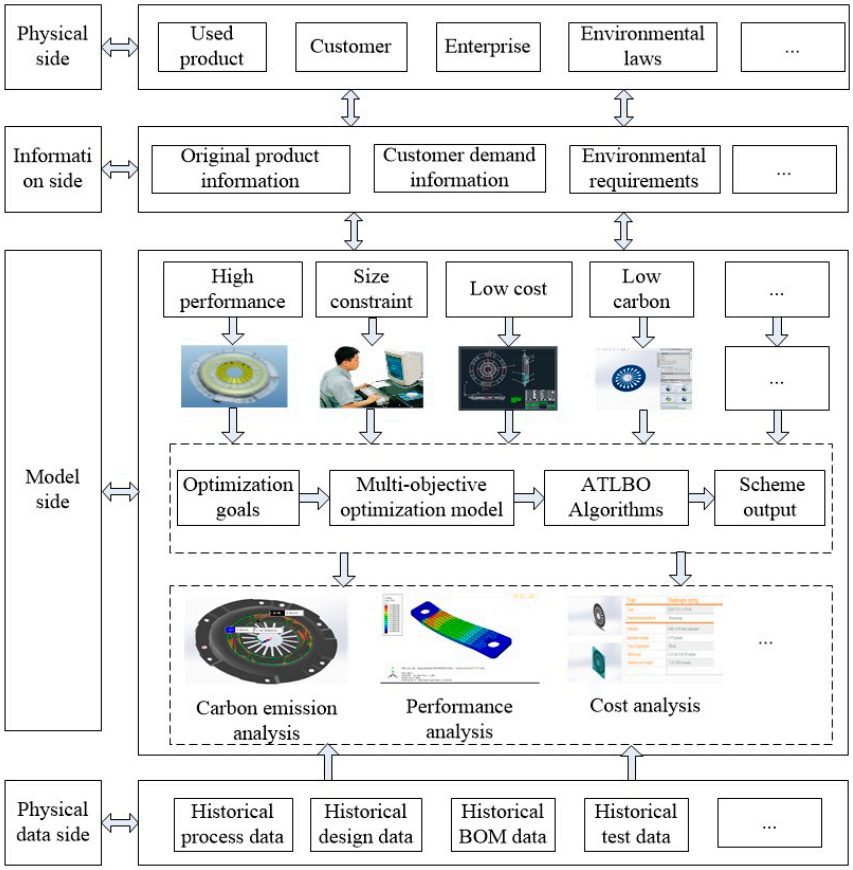

Figure 1. Integrated design framework for remanufacturing process.

(1) External constraint information obtention

The external constraint information of the DFRP contains original product information, customer demand information, enterprise remanufacturing demand information, environmental protection legislation and regulations, etc., constituting the constraints and design objectives for the realization of the remanufacturing process scheme. The information mentioned above can be mainly generalized into three respects: performance request, cost request, energy saving and emission reduction, and so on. By analyzing the intrinsic con-

nection between the target information and the remanufacturing process parameters, the mapping mathematical model between the two is established, which provides a convenient way to optimize the process parameters.

(2) Performance requirements of the remanufactured product

Performance requirements mainly include the hardness, strength, and corrosion resistance of the remanufactured products, which determine whether the remanufactured products can be competitive in the market. And the remanufacturing process parameters directly determine whether or not these properties will be met. Wherein, whether the remanufacturing process parameters meet the requirements can be verified through virtual simulation technology and the real-time adjustment of the process parameters to meet the performance requirements.

(3) Remanufacturing cost

The remanufacturing cost determines the profitability of the manufacturer or remanufacturer, as well as the cost-effectiveness and market value of the remanufactured product. Therefore, the remanufacturing process scheme needs to consider the costs of the remanufacturing process. Remanufacturing costs consist of material costs, energy costs, processing costs, contracted processing costs, and additional costs. In the real remanufacturing process, the situation of exceeding the predetermined cost may occur, so remanufacturing process parameters need to be reasonably adjusted to decrease the remanufacturing cost.

(4) Environmental requirements

The remanufacturing process conserves energy including electricity, water, and oil and produces a large number of pollutants such as wastewater, metal waste, and waste oil. Based on the regulations and laws on energy conservation and emission reduction policies and the dual-carbon goal, the energy consumption and emissions of these two parts must be significantly reduced. In order to symbolize the target of energy conservation and emission reduction, carbon emissions are available to express the energy consumption of the remanufacturing process and the waste treatment process.

The optimization objective of the remanufacturing process scheme is analyzed by extracting the constraint information, and it is the key to the optimization of the remanufacturing process scheme to establish the correlation between the constraint information and the process parameters, while the process of establishing each mapping relationship is as follows.

(1) The mapping relationship between the performance and remanufacturing process parameters

Performance consists of product rigidity, component strength, hardness, etc. There is a mapping connection between performance and process parameters that is obtained through experience equations or determinants. Universal functional equations between the two are described by the process matrices of the axiomatic design, as follows:

$$\begin{Bmatrix} F_1 \\ F_2 \\ \dots \\ F_m \end{Bmatrix} = \begin{bmatrix} C_{11} & C_{12} & \dots & C_{1j} & \dots & C_{1n} \\ C_{21} & C_{22} & \dots & C_{2j} & \dots & C_{2n} \\ \dots & \dots & \dots & \dots & \dots & \dots \\ C_{i1} & C_{i2} & \dots & C_{ij} & \dots & C_{in} \\ \dots & \dots & \dots & \dots & \dots & \dots \\ C_{m1} & C_{m2} & \dots & C_{mj} & \dots & C_{mn} \end{bmatrix} \begin{Bmatrix} PV_1 \\ PV_2 \\ \dots \\ PV_n \end{Bmatrix} \quad (1)$$

where F_m indicates the m-th performance of the product, PV_n indicates the n-th process parameter, while C_{ij} indicates the mapping function between the i-th performance and the j-th process parameter, either as a true number or as a functional formula.

(2) The mapping relationship between the remanufacturing costs and process parameters

Technicians develop remanufacturing process schemes according to customer requirements and have them processed by the remanufacturing workshop. The process scheme directly determines the energy consumption of electricity, water, materials, and other energy sources in the remanufacturing process. Higher consumption definitely increases the cost of remanufacturing. Every process parameter contains different machining paradigms, each utilizing the appropriate machining equipment, raw materials, and heat treatments. Various remanufacturing process schemes will consume varying levels of energy. Therefore, it is essential to analyze the remanufacturing cost based on the particular scrap and customer requirements. To address the relationship between remanufacturing costs and process parameters, the least-squares method is applied to perform a linear fit of the functional relationship between the two, which is shown in the figure below:

$$M_i = F_1(PV_i, b) = a_i \cdot PV_i + b_i \tag{2}$$

$$E_j = F_2(PV_j, b) = a_j \cdot PV_j + b_j \tag{3}$$

$$C_o = \sum_{p=1}^{q} M_p c_p + \sum_{q=1}^{n} E_q c_q \tag{4}$$

In Equation (2), M_i denotes the material conservation of the i-th process parameter, and in Equation (3), E_j denotes the energy conservation of the ith process parameter. In Equation (4), M_p indicates the quality of the p-th expended material, c_p denotes the price of the pth material, and E_q indicates the quantity of the q-th energy consumed and the price of the j-th energy.

(3) The mapping relationship between carbon emissions and remanufacturing process parameters

The carbon emissions from the remanufacturing process have direct relevance to the remanufacturing process scheme. The remanufacturing process mainly consists of remanufacturing modes and process paths in terms of dimensional restoration, performance restoration, structural upgrading, and performance upgrading, which can produce carbon emissions. Carbon emissions mainly come from the consumption of electricity, water, raw materials, and natural gas. The remanufacturing carbon emission boundary is shown in Figure 2.

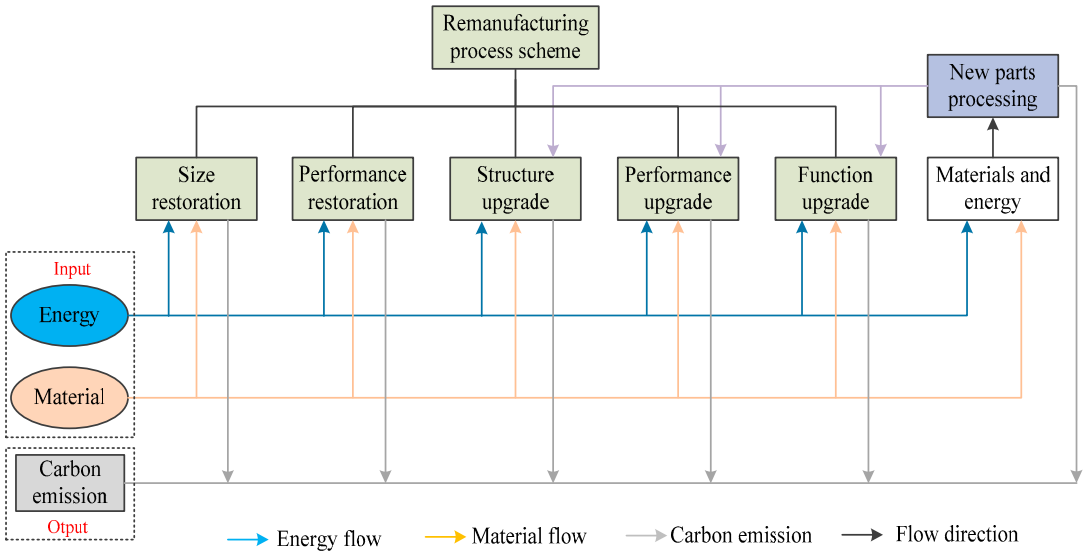

Figure 2. Remanufacturing carbon emission boundary.

It is first necessary to establish a carbon emission calculation model, then the sensitivity analysis can be utilized to develop a mapping relationship between carbon emissions and the remanufacturing process parameters. The details are as follows.

$$H_i = \sum_{q=1}^{p} N_q^E \, f_q^E + \sum_{t=1}^{n} N_t^M \, f_t^M \tag{5}$$

$$N_i = f_{N_i}(PV_i) \tag{6}$$

$$S_i = \frac{\partial N_i}{\partial PV_i} = \frac{\partial f_{N_i}(PV_i)}{\partial PV_i} \tag{7}$$

$$\Delta N_i = S_i \cdot \Delta PV_i \tag{8}$$

$$N_i = S_i \cdot PV_i + g_i \tag{9}$$

$$H_i = \sum_{q=1}^{p} (S_q \cdot PV_i + g_q) f_q^E + \sum_{t=1}^{n} (S_t \cdot PV_i + g_t) f_t^M \tag{10}$$

In Equation (5), H_i represents the carbon emissions corresponding to the i-th remanufacturing process parameter, N_{qi}^E represents the q-th energy consumption, f_q^E represents the carbon emission factor of the q-th energy, and S_i indicates the sensitivity coefficient between the i-th remanufacturing process parameter and the corresponding carbon emissions. Equation (8) represents the functional relationship between changes in energy consumption and subtle changes in design parameters. By solving Equation (8), and the result is shown in Equation (9), g_i represents the constant of the i-th carbon emission equation, f_q^E represents the carbon emission factor of the q-th energy source, and f_t^M represents the carbon emission factor of the t-th material.

In Equation (5), H_i denotes the carbon emissions corresponding to the i-th remanufacturing process parameter, N_{qi}^E denotes the q-th energy conservation, f_q^E denotes the carbon emission coefficient of the q-th energy source, and S_i denotes the sensitivity coefficient between the i-th remanufacturing process parameter and the respective carbon emissions. Equation (8) indicates the functional relationship between changes in energy consumption and subtle changes in design parameters. By solving Equation (8), the results are displayed in Equation (9), where g_i indicates the normal of the i-th carbon emission equation, f_q^E indicates the carbon emission coefficient of the q-th energy resources, and f_t^M indicates the carbon emission coefficient of the t-th material.

2.2. Mathematical Modeling for Adaptive Optimization of the DFRP

The DFRP is a process of continuous feedback and optimization based on the customer, processing, quality, and assembly to obtain the best design solution. Therefore, process engineers need to adjust the preliminary remanufacturing process scheme to approach the optimal process parameters. However, the optimization process is then cumbersome, time-consuming, and costly, and it is not even possible to obtain optimal parameters for the remanufacturing process. To increase the success rate of optimization, the virtual simulation model of the process scheme can be established, using solid modeling, CAE simulation, and energy consumption assessment and other technologies for the virtual validation of the process scheme. The validation results will be fed back to the main departments of the requirements, which will compare and analyze them based on the historical physical data, and feed the analysis results of the design objectives into the optimization process until the optimal design results are obtained. The specific optimization methods are shown in Figure 3.

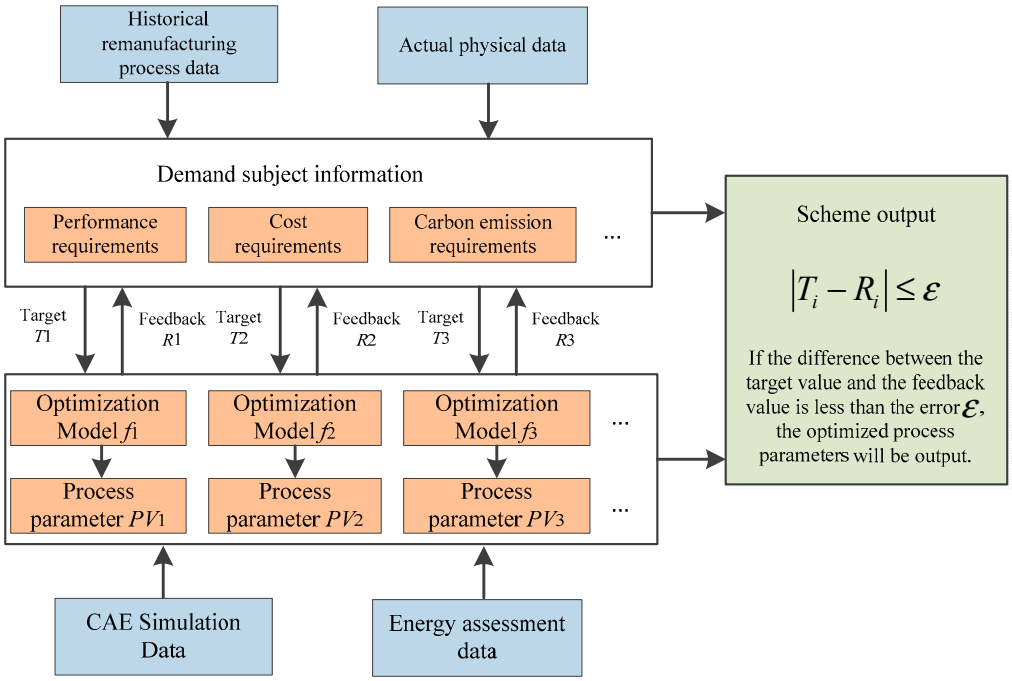

Figure 3. Adaptive optimization model for DFRP.

Firstly, it is necessary to construct a multi-objective optimization model for the remanufacturing process scheme, mainly focusing on three objectives: performance, remanufacturing cost, and remanufacturing carbon emissions. The specific details are as follows:

$$\min F_i = \frac{1}{C_{ij} \cdot PV_i} \tag{11}$$

$$\begin{aligned} C_{oi} &= \sum_{p=1}^{q} (a_p \cdot PV_i + b_p) c_p + \sum_{q=1}^{k} (a_q \cdot PV_i + b_q) c_q \\ \min C_o &= \sum_{i=1}^{n} C_{oi} = \sum_{i=1}^{n} \left(\sum_{p=1}^{q} (a_p \cdot PV_i + b_p) c_p + \sum_{q=1}^{k} (a_q \cdot PV_i + b_q) c_q \right) \end{aligned} \tag{12}$$

$$\min H = \sum_{i=1}^{n} \left(\sum_{q=1}^{p} (S_q \cdot PV_i + g_q) f_q^E + \sum_{t=1}^{n} (S_t \cdot PV_i + g_t) f_t^M \right) \tag{13}$$

where F_i denotes the i-th performance goal of the remanufactured product, C_{oi} denotes the remanufacturing cost consumed by the i-th process parameter, C_{oi} denotes the total remanufacturing cost, and H denotes the total remanufacturing carbon emission.

The constraints of the optimization model are set according to the system requirements as well as legal policies as follows.

$$C_s < C_o < C_d \tag{14}$$

$$H < H_l \tag{15}$$

$$PV_{lp} \leq PV_i \leq PV_{up} \tag{16}$$

In Equation (16), C_s represents the constraint value of the remanufacturer on the remanufacturing cost, and C_d represents the constraint value proposed by the customer for the remanufacturing cost. Generally, the remanufacturer's set remanufacturing cost will be lower than the customer's set remanufacturing cost. H_l indicates the carbon emission limit specified by policies and regulations. PV_{lp} and PV_{up} are the lower and upper limits of the process parameters, respectively, mainly determined by factors such as product system constraints and tolerance ranges.

2.3. Optimization Model Solution for DFRP

The way to solve the multi-objective optimization model has been developed very maturely, and the most widely used algorithms are the particle swarm optimization algorithm, genetic algorithm, ant colony algorithm, etc. However, none of these algorithms have the problems of insufficient computational accuracy and poor stability. Aiming at the restrictions of former algorithms, an adaptive teaching-based optimization algorithm (ATLBO) was developed. This algorithm imitates the process of students learning from teachers. It can adaptively adjust the learning method to achieve faster learning after learning a certain amount of knowledge. It can avoid entering the local optimum too early, improve the global search ability, speed up the solution speed, and react faster to optimization model variation. The process of the ATLBO algorithm is shown in Figure 4.

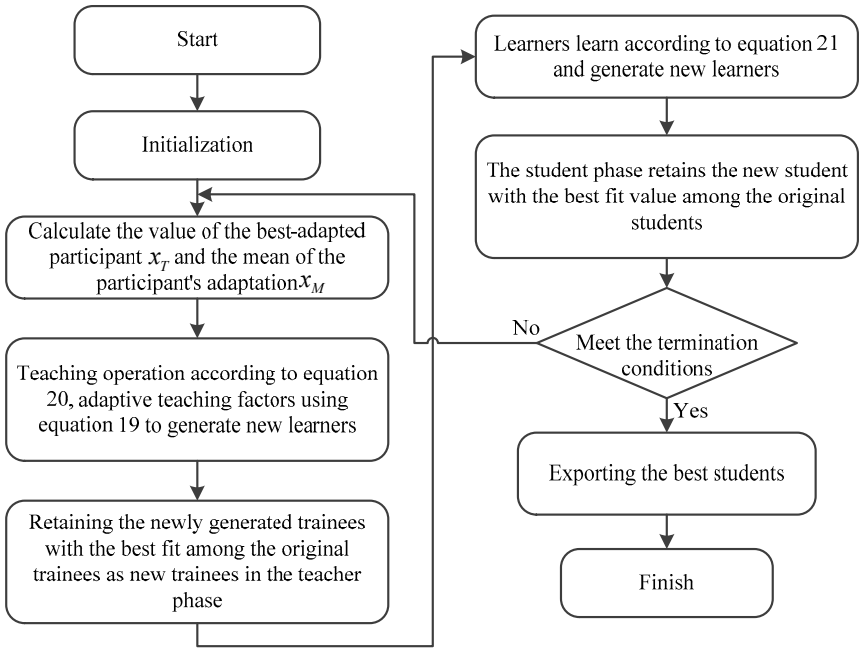

Figure 4. Adaptive teaching–learning-based optimization algorithm process.

(1) Teacher stage

In the teaching stage, there is variability in the level of teachers and students, and learning ability is used to measure the difference in learning between the two, then the average degree of difference in learning ability between teachers and students is calculated as follows.

$$dif = T_c(t) \cdot (x_T - \theta \cdot x_M) \tag{17}$$

$$\theta = round(1 + rand(0,1)) \tag{18}$$

$$T_c(t) = \frac{1}{2}\left[(T_{c\max} - T_{c\min}) \cdot \left(\frac{t_{\max} - t_i}{t_{\max}}\right)^2 + (T_{c\max} - T_{c\min}) \cdot \left(\frac{t_{\max} - t_i}{t_{\max}}\right)\right] + T_{c\min} \tag{19}$$

In Equation (17), x_M denotes the average value of the M-th student, x_T denotes the average value of the teacher, $T_c(t)$ denotes the adaptive learning factor, $T_{c\max}$ denotes the maximum value of the learning factor, $T_{c\min}$ denotes the minimum value of the learning factor, t_i denotes the number of iterations in the learning process, and $t_{\max}$ denotes the maximum number of iterations.

Moreover, students are allowed to learn based on the variability of their learning ability with respect to their teachers, which is calculated as shown in the formula below.

$$x_{inew} = x_i + dif \tag{20}$$

In Equation (20), x_i represents the value of the i-th student before learning, and x_{inew} represents the value of the i-th student after learning.

(2) Student stage

At the student stage, each student randomly takes a learning object in the class according to their learning ability for comparing and analyzing; meanwhile, the learning coefficient is adjusted according to the ability gap between the two. The details of the calculation method are as follows.

$$x_{inew} = \begin{cases} x_i + rand(0,1)\cdot(x_i - x_j) & f(x_i) > f(x_j) \\ x_i + rand(0,1)\cdot(x_j - x_i) & f(x_i) < f(x_j) \end{cases} \quad (21)$$

(3) Ending criteria

If the optimization process achieves the maximum number of iterations, the calculation is aborted, and the optimized design parameters are outputted. Alternatively, the calculation steps 1 and 2 are repeated.

3. Case Study

Taking the DFRP of turbine blades as an example for the analysis, the turbine blades have a length of 20 mm, a thickness of 3 mm, and a maximum diameter of 50 mm. As the core power component of a turbine rotor, turbine blades have complex physical structures, long manufacturing cycles, and are difficult to manufacture. As the turbine blade has a complex form and structure, together with the effects of working conditions, raw materials, and construction, it is easy to cause fatigue damage, wear, and fracture on the surface of the turbine blade under the action of centrifugal, aerodynamic, and temperature loads. The physical drawing of the turbine blade is shown in Figure 5. Therefore, the quality department proposed a remanufacturing process scheme to address the above-mentioned issues, whereby, for responding to the "dual-carbon policy", it is important for the process scheme to satisfy the requirements of low-carbon remanufacturing. In addition, the remanufacturing company needs to control the remanufacturing cost to ensure profitability. Hence, it is essential to establish matrix models between cavity surface strength and process parameters, remanufacturing cost and process parameters, and carbon emission and process parameters, which are shown in Figure 5.

Figure 5. Physical diagram of turbine blade failure.

Firstly, to repair the surface wear of the turbine blade, laser cladding can be used to modify the surface of the cavity. The amount of carburization during laser cladding directly affects the repair performance of the turbine blade. Based on the empirical formula, the relationship between the carburization and the tensile strength of the turbine blade can be obtained, as shown below.

$$\sigma_b = 300(1 - PV_1/0.83) + 1000(PV_1/0.83) \quad (22)$$

In Equation (22), σ_b denotes the tensile strength of the mold cavity, and PV_1 denotes the degree of the carburization of the turbine blade.

The sensitivity of the relationship between carbon emissions and process parameters was derived from the energy consumption and material consumption in the remanufacturing process scheme as well as from historical manufacturing data, and the carbon emission sensitivity is calculated using the cavity surface carburization as an example; the details are shown in Table 1.

Table 1. Carbon emission factors for different energy sources and materials.

Serial Number	Energy or Materials	Carbon Emission Factor
1	Electric energy	0.801 ($kgCO_2/kW \times h$)
2	Lube	2.95 ($kgCO_2/L$)
3	Steel	7.084 ($kgCO_2/kg$)
4	Natural gas	2.162 ($kgCO_2/m^3$)
5	Water	0.194 ($kgCO_2/kg$)
6	Aluminum	9.677 ($kgCO_2/kg$)

The laser cladding of the turbine blade will consume a large amount of electricity, water, and natural gas. The specific consumption and carbon emissions are shown in Table 2.

Table 2. Energy and material consumption.

Process Parameter	Energy and Material	Consumption	Carbon Emission Value
Carburization in the cavity (PV_1)	Electric energy	1.1313 kW × h	9.581 $kgCO_2$
	Water	0.8 kg	
	Natural gas	0.0075 m^3	
	Steel	1.2 kg	

The sensitivity to carbon emissions of the process parameters was calculated based on Equations (7) and (8). The sensitivity to minor variations in the process parameters was calculated using used turbine blades of this type as a reference, and the results are presented in Table 3.

Table 3. Sensitivity analysis results of process parameters and carbon emission.

Process Parameter	Standard Carburizing Amount	Carbon Emission	Sensitivity Value S
Carburization (PV_1)	0.3%	9.581 $kgCO_2$	−0.1302

From Table 3, it can be seen that PV_1 has a negative association with carbon emissions, and the functional correlation between carbon exudation and carbon emissions can be summarized as follows.

$$H_1 = -0.1302PV_1 + 1.1206$$

The remanufacturing cost is related to the energy and material consumption of mold laser cladding, and the remanufacturing process parameters directly affect their consumption. Therefore, the least-squares method can be used to construct a direct functional relationship between remanufacturing costs and remanufacturing process parameters. The specific calculation process is shown in Table 4.

Table 4. Remanufacturing cost.

Process Parameter	Energy and Material	Consumption	Price	Remanufacturing Cost
Carburization in the cavity (PV_1)	Electric energy	1.1313 kW × h	0.14 USD/kW × h	USD 0.158
	Water	0.8 kg	0.00057 USD/kg	USD 0.00046
	Natural gas	0.0075 m^3	0.354 USD/m^3	USD 0.0027
	Steel	1.2 kg	0.49 USD/kg	USD 0.59

Based on historical laser cladding cost data, the least-squares method was applied to fit the functional relationship between remanufacturing costs and process parameters. The remanufacturing cost function can be calculated according to Equations (2)–(4). Then, the parameters of the remanufacturing cost function were calculated as shown in Table 5.

Table 5. Sensitivity analysis results of process parameters and remanufacturing cost.

Process Parameter	Standard Carburizing Amount	Actual Carburizing Amount	*a*	*b*
Carburization (PV_1)	0.3%	0.5%	3.9985	−0.06825
			3.5	−0.25
			0.035	−0.003
			5	−0.3

According to Equation (4), the cost function of turbine blade remanufacturing can be obtained, as shown below.

$$C_o = 21.6014PV_1 - 1.126865$$

The multi-objective optimization model for the remanufacturing process scheme related to performance, cost, and carbon emissions is as follows.

$$\begin{cases} \min F_1 = \frac{1}{\sigma_b} = \frac{1}{300(1-PV_1/0.83)+1000(PV_1/0.83)} \\ \min C_o = 21.6014PV_1 - 1.126865 \\ \min H_1 = -0.1302PV_1 + 1.1206 \end{cases}$$

s.t.

$$0.28\% \leq PV_1 \leq 0.6\%$$

According to the above rules, the constraint range of PV_1 can be obtained, while the range of carbon content PV_1 can be acquired by looking up the characteristics of the 45 # steel material.

The ATLBO was adopted to resolve to the multi-objective optimization model of the remanufacturing process scheme, where the number of students was fixed at 10, where the number of students' study courses was fixed at 1 (the number of process variables), and where the number of iterations was fixed at 50. To demonstrate the superiority of the ATLBO, the conventional Teaching- and Learning-Based Optimization Algorithm (TLBO) was simultaneously performed and a comparison of the results was conducted, and the results of the calculations are shown in Figures 6–8.

The three figures above are able to visualize the computational process, results, and quality of the two algorithms, thus reflecting which of the two algorithms is superior.

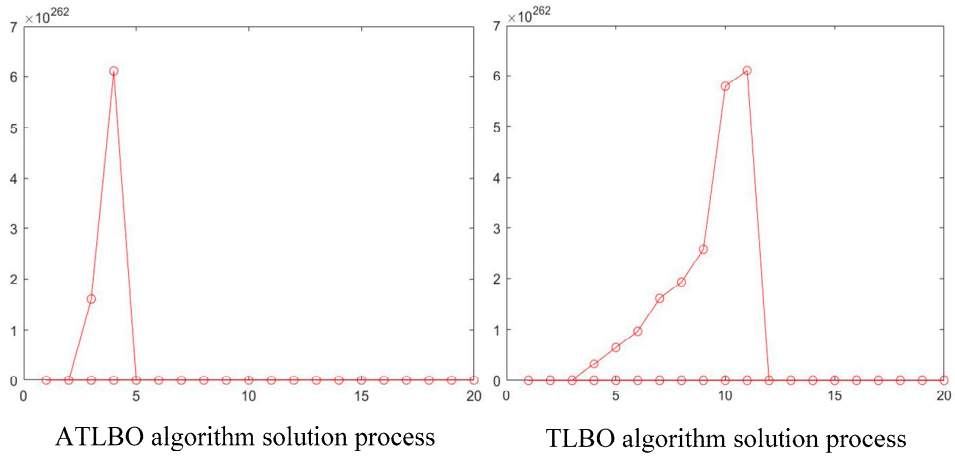

Figure 6. Comparison between ATLBO and TLBO algorithm solution process.

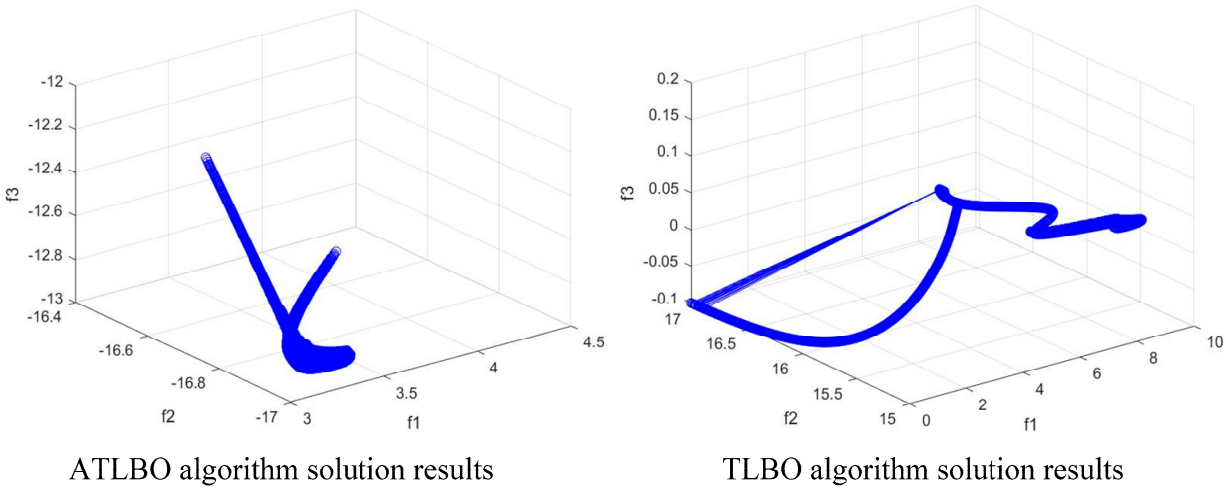

Figure 7. Comparison of the solution results of ATLBO and TLBO algorithms.

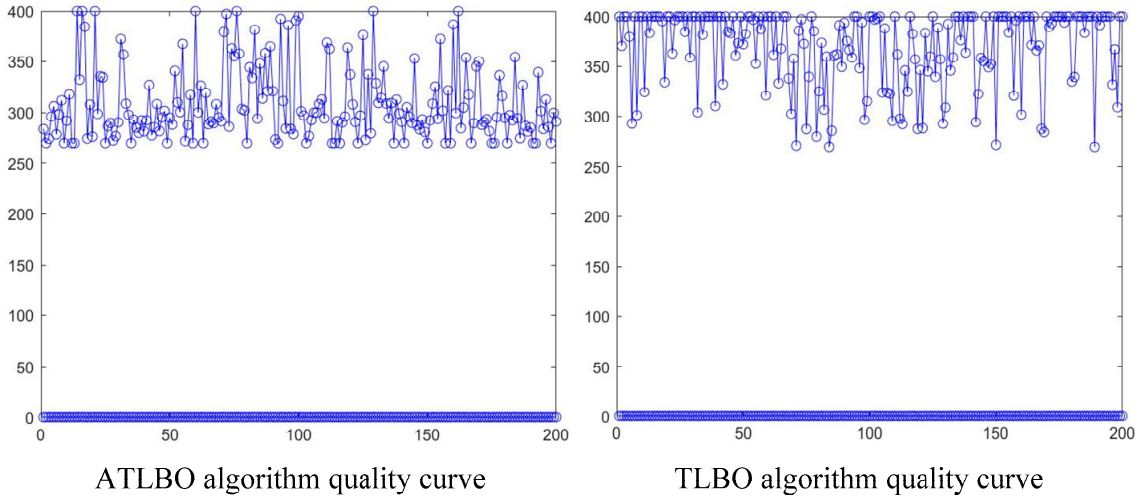

Figure 8. Comparison of solution quality between ATLBO and TLBO algorithms.

4. Results and Discussion

From Figure 6, it is shown that the ATLBO algorithm converged at the 5th step of the multi-objective function iteration, while the TLBO algorithm converged at the 12th

step of the multi-objective function iteration, which meant that the ATLBO algorithm was faster. From Figure 7, it can be seen that the ATLBO algorithm was faster than the TLBO algorithm and had a better convergence. From Figure 8, it can be seen that the ATLBO tended to stabilize the quality value of the solution process, and the fluctuation state tended to stabilize at the end of the iteration, whereas the quality value of the TLBO was in a fluctuating status and unable to be stabilized. The reason was that the ATLBO constantly adjusted the learning strategy during the solving process, which could solve the objective function in a stabilized and faster way. The solution results are shown in Table 6.

Table 6. Comparison of optimization results of process parameters.

Algorithms	Process Parameter	Carbon Emission	Remanufacturing Cost	Tensile Strength
	PV_1			
ATLBO	0.32%	10.5481 $kgCO_2$	USD 0.681	455.67 Mpa
TLBO	0.35%	11.6806 $kgCO_2$	USD 0.733	450.62 Mpa

However, compared to the TLBO algorithm, the ATLBO algorithm reduced carbon emissions by 11.7%, lowered the in-house remanufacturing cost of the turbine blade by USD 0.052, and slightly improved tensile strength. Overall, the ATLBO algorithm delivered a superior, quicker solution to the process parameters than the TLBO algorithm did.

For verifying the dependability of the optimization scheme, the process scheme was verified using virtual simulation technology. First of all, SolidWorks 2020 software was utilized to establish a three-dimensional model of the turbine blade, and the sustainable development module was employed to calculate the carbon emission and remanufacturing cost in the remanufacturing process of the turbine blade. The performance of the turbine blade was simulated using ANSYS 2020 software, and the detailed results are shown in Figure 7.

As shown in Figure 9, the ANSYS software analyzed that the maximum stress of the turbine blade under a load of 459.15 Mpa, which was basically consistent with the results obtained by the ATLBO algorithm. As shown in Figure 10, the sustainability module of SolidWorks 2020 software calculated the carbon emissions of the remanufacturing process to be 11 $kgCO_2$, which was essentially the same as that calculated by the ATLBO algorithm. As shown in Figure 11, the cost analysis module of the SolidWorks software calculated that the remanufacturing cost of turbine blades was USD 7.05. In contrast, the manufacturer's cost containment requirement was not to exceed USD 10 (excluding labor, facility, and administrative costs). As a result, the total cost of remanufacturing was lower than the remanufacturer's anticipated maximum cost.

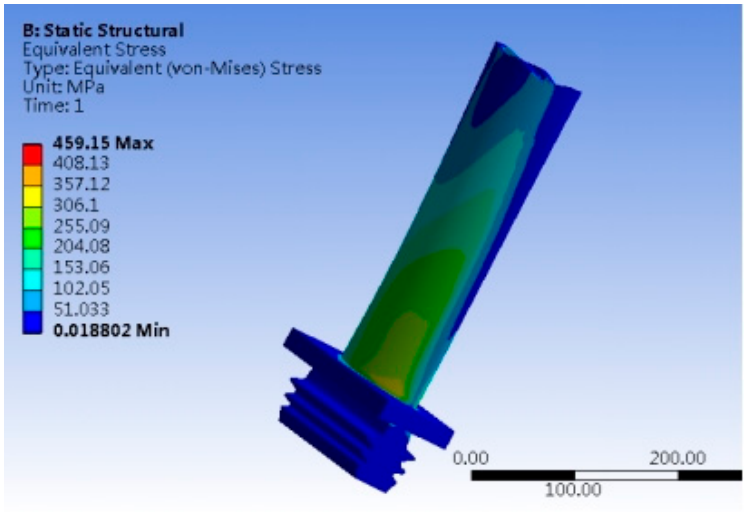

Figure 9. Stress distribution in the turbine blade.

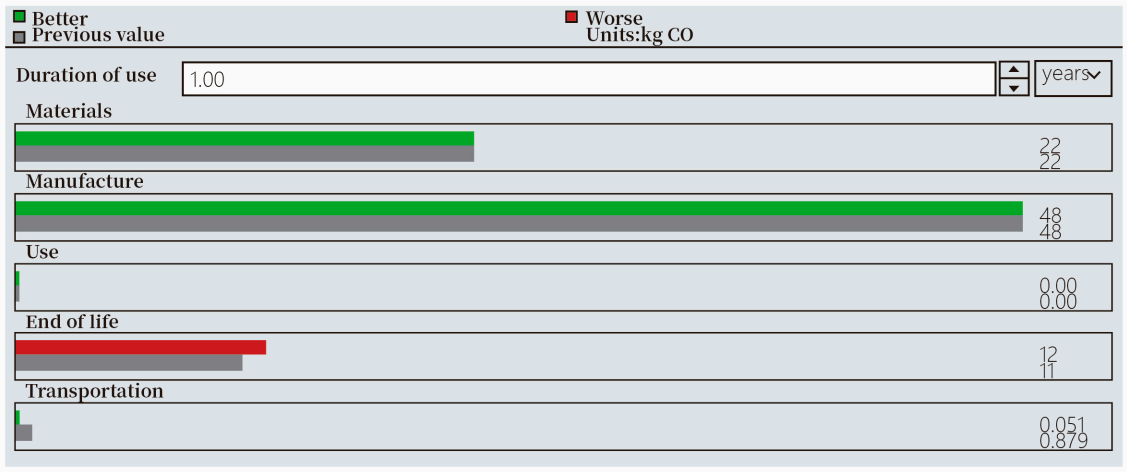

Figure 10. Carbon emission from turbine blade remanufacturing.

Cost analysis

Materials:	8.90 USD	55.8%
Remanufacturing:	7.05 USD	44.2%
Label:	0. 00 USD	0%

Figure 11. Remanufacturing cost of turbine blade.

The used turbine blade was repaired according to the carburization parameters of the remanufacturing process scheme. As shown in Figure 12, laser cladding was applied to repair the used turbine blade, and as shown in Figure 13, the broken part of the turbine blade was completely repaired.

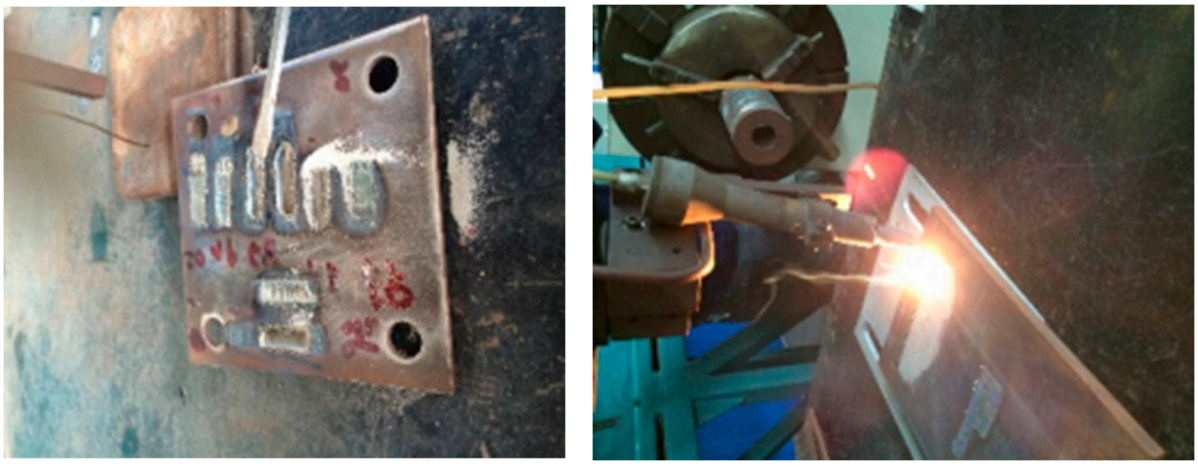

Figure 12. Laser cladding remanufacturing of turbine blade.

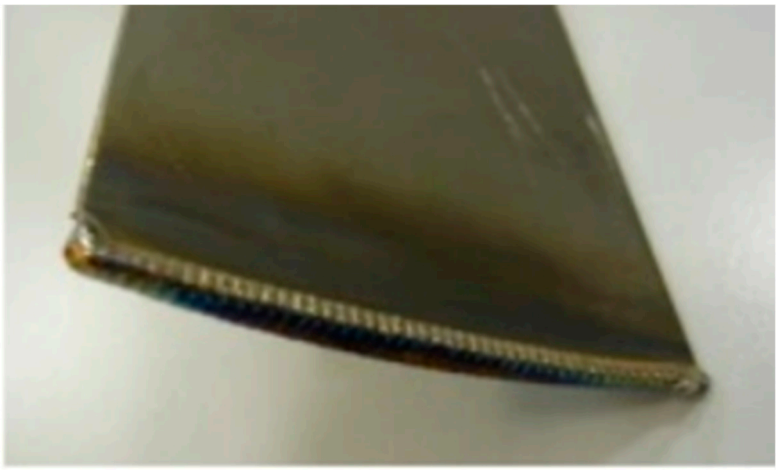

Figure 13. Repaired turbine blades.

Overall, in comparison to conventional TLBO algorithms, the ATLBO was able to optimize remanufacturing process parameters faster and more rationally, providing a more feasible process scheme. Then, compared with the initial carburization parameter, the optimized carbon content parameters could meet the tensile strength of turbine blades and could also reduce remanufacturing carbon emissions and costs. When the carburization parameter of the turbine blades reached 0.3%, the repair work was basically completed, and the tensile strength also reached the optimal value. Otherwise, when the carburization parameter of turbine blades reached 0.35%, the tensile strength did not increase but decreased. This was because if the carburization parameter exceeded a certain threshold, the hardness of the blades increased, the toughness decreased, and the tensile strength also decreased. Therefore, selecting the appropriate carburization parameter for laser cladding is the key to energy conservation, emission reduction, and improving tensile strength.

5. Conclusions and Future Work

The design for the remanufacturing process is essential to influence the carbon emission, performance, and cost of remanufacturing used products. In order to produce a reasonable remanufacturing process solution to decrease carbon emission and cost and recover the performance of used products, it is essential to establish a mapping model between the remanufacturing process parameters and remanufacturing carbon emission, cost, and performance. In addition, this mapping model can be used to solve the optimal remanufacturing process parameters using an optimization algorithm to achieve the remanufacturing objectives. Therefore, an integrated design method for the remanufacturing process based on a multi-objective optimization model was proposed in this research. Moreover, the results showed that the mapping model established the correlation between the remanufacturing process parameters and remanufacturing carbon emission, cost, and performance, which contributed to the theoretical basis for the development of a multi-objective remanufacturing process scheme. Furthermore, the remanufacturing process scheme optimization model and algorithm proposed in this research can effectively generate a remanufacturing process solution that meets the multi-objective requirements and design constraints, which can significantly reduce the remanufacturing carbon emission and cost and improve the performance of used products. In general, applying this method to the large-scale remanufacturing industry will significantly reduce global remanufacturing carbon emissions, greatly mitigate the global greenhouse effect, and improve the global ecological environment, while greatly reducing the remanufacturing costs of enterprises and improving the performance of used products.

For future work, there is a need to develop an intelligent method that can quickly simulate optimized process solutions and verify their feasibility. Digital twin technology can realistically depict the remanufacturing process of used products and make real-time

corrections to the process parameters based on the remanufacturing process data, which can help designers optimize the remanufacturing process scheme more intuitively and faster, which will be investigated in the future. Moreover, it is necessary to consider process design methods in multiple remanufacturing modes, such as the remanufacturing upgrade mode, or the hybrid mode of repair and upgrade, to make the remanufacturing process design methods more applicable.

Author Contributions: Software, M.G.; formal analysis, Y.C.; resources, Y.L.; writing—original draft, C.K.; writing—review and editing, Q.J. All authors have read and agreed to the published version of the manuscript.

Funding: This work was supported by the Wuhan Institute of Technology Research Foundation Project [K2023018] and the Sustainable Design and Product Ecological Innovation Team Project. These financial contributions are gratefully acknowledged.

Data Availability Statement: All data are contained within the article.

Conflicts of Interest: The authors declare no conflicts of interest.

References

1. Ai, X.; Jiang, Z.; Zhang, H.; Wang, Y. Low-carbon product conceptual design from the perspectives of technical system and human use. *J. Clean. Prod.* **2020**, *244*, 118819. [CrossRef]
2. Jiang, Z.; Ding, Z.; Liu, Y.; Wang, Y.; Hu, X.; Yang, Y. A data-driven based decomposition-integration method for re-manufacturing cost prediction of end-of-life products. *Robot. Comput.-Integr. Manuf.* **2020**, *61*, 101838. [CrossRef]
3. Ke, C.; Jiang, Z.; Zhang, H.; Wang, Y.; Zhu, S. An intelligent design for remanufacturing method based on vector space model and case-based reasoning. *J. Clean. Prod.* **2020**, *277*, 123269. [CrossRef]
4. Tolio, T.; Bernard, A.; Colledani, M.; Kara, S.; Seliger, G.; Duflou, J.; Battaia, O.; Takata, S. Design, management and control of demanufacturing and remanufacturing systems. *CIRP Ann.-Manuf. Technol.* **2017**, *66*, 585–609. [CrossRef]
5. Ke, C.; Jiang, Z.; Zhu, S.; Wang, Y. An integrated design method for remanufacturing process based on performance demand. *Int. J. Adv. Manuf. Technol.* **2022**, *118*, 849–863. [CrossRef]
6. Chen, D.; Jiang, Z.; Zhu, S.; Zhang, H. A knowledge-based method for eco-efficiency upgrading of remanufacturing process planning. *Int. J. Adv. Manuf. Technol.* **2020**, *108*, 1153–1162. [CrossRef]
7. Jiang, Z.; Jiang, Y.; Wang, Y.; Zhang, H.; Cao, H.; Tian, G. A hybrid approach of rough set and case-based reasoning to remanufacturing process planning. *J. Intell. Manuf.* **2019**, *30*, 19–32. [CrossRef]
8. Jiang, Z.; Ding, Z.; Zhang, H.; Cai, W.; Liu, Y. Data-driven ecological performance evaluation for remanufacturing process. *Energy Convers. Manag.* **2019**, *198*, 111844. [CrossRef]
9. Jiang, X.; Tian, Z.; Liu, W.; Tian, G.; Gao, Y.; Xing, F.; Suo, Y.; Song, B. An energy-efficient method of laser remanufacturing process. *Sustain. Energy Technol. Assess.* **2022**, *52*, 102201. [CrossRef]
10. Ke, C.; Pan, X.; Wan, P.; Jiang, Z.G.; Zhao, J.J. An integrated design method for used product remanufacturing scheme considering carbon emission. *Sustain. Prod. Consum.* **2023**, *41*, 348–361. [CrossRef]
11. Jiang, Z.; Zhou, T.; Zhang, H.; Wang, Y.; Cao, H.; Tian, G. Reliability and cost optimization for remanufacturing process planning. *J. Clean. Prod.* **2016**, *135*, 1602–1610. [CrossRef]
12. Zhao, J.; Xue, Z.; Li, T.; Ping, J.; Peng, S. An energy and time prediction model for remanufacturing process using graphical evaluation and review technique (GERT) with multivariant uncertainties. *Environ. Sci. Pollut. Res.* **2023**, 1–13. [CrossRef] [PubMed]
13. Ramírez, F.J.; Aledo, J.A.; Gamez, J.A.; Pham, D.T. Economic modelling of robotic disassembly in end-of-life product recovery for remanufacturing. *Comput. Ind. Eng.* **2020**, *142*, 106339. [CrossRef]
14. Shi, J.; Xu, H.; Shu, F.; Ren, M.; Lu, Z. A PCA-based method for remanufacturing process optimization from sustainability aspects. *Int. J. Ind. Eng.-Theory Appl. Pract.* **2023**, *30*, 986–998.
15. Peng, H.; Wang, H.; Chen, D. Optimization of remanufacturing process routes oriented toward eco-efficiency. *Front. Mech. Eng.* **2019**, *14*, 422–433. [CrossRef]
16. Liu, C.; Zhu, Q.; Wei, F.; Rao, W.; Liu, J.; Hu, J.; Cai, W. An integrated optimization control method for remanufacturing assembly system. *J. Clean. Prod.* **2020**, *248*, 119261. [CrossRef]
17. Liu, Q.T.; Shang, Z.Y.; Ding, K.; Guo, L.; Zhang, L. Multi-process routes based remanufacturability assessment and associated application on production decision. *J. Clean. Prod.* **2019**, *240*, 118114. [CrossRef]
18. Cavique, L.; Cavique, M.; Mendes, A.; Cavique, M. Improving information system design: Using UML and axiomatic design. *Comput. Ind.* **2022**, *135*, 103569. [CrossRef]
19. Chen, J.; Tang, J.; Yang, D. Study on sensitivity analysis of tooth surface roughness parameters and contact stress. *J. Northwestern Polytech. Univ.* **2022**, *40*, 883–891. [CrossRef]

20. Zhang, X.; Ao, X.; Jiang, Z.; Zhang, H.; Cai, W. A remanufacturing cost prediction model of used parts considering failure characteristics. *Robot. Comput. Manuf.* **2019**, *59*, 291–296. [CrossRef]
21. Zhang, X.; Liu, C.; Zhao, B. An optimization research on groove textures of a journal bearing using particle swarm optimization algorithm. *Mech. Ind.* **2021**, *22*, 1. [CrossRef]
22. Xue, D.; Imaniyan, D. An Integrated Framework for Optimal Design of Complex Mechanical Products. *J. Comput. Inf. Sci. Eng.* **2021**, *21*, 041004. [CrossRef]
23. Tao, X.R.; Pan, Q.K.; Gao, L. An efficient self-adaptive artificial bee colony algorithm for the distributed re-source-constrained hybrid flowshop problem. *Comput. Ind. Eng.* **2022**, *169*, 108200. [CrossRef]
24. Mi, X.; Liao, Z.; Li, S.; Gu, Q. Adaptive teaching–learning-based optimization with experience learning to identify photovoltaic cell parameters. *Energy Rep.* **2021**, *7*, 4114–4125. [CrossRef]